# Characterization of Low Loss Waveguides Using Bragg Gratings

Yi-Wen Hu, Yang Zhang, Pradip Gatkine, Joss Bland-Hawthorn, Sylvain Veilleux, and Mario Dagenais, *Fellow, IEEE*

***Abstract*—A novel approach is developed for measuring small losses in highly transparent $Si_3N_4/SiO_2$ waveguides on a silicon chip. The approach is particularly applicable to waveguides written by high-resolution patterning techniques, such as e-beam lithography, whose lengths cannot be easily increased beyond several centimeters. This method is based on measuring the transmission of an optical cavity formed by two highly reflective (*R* at least 0.999) simple Bragg gratings and a uniform waveguide between the two gratings whose length can be varied to increase the loss fitting accuracy. A theoretical model based on an ABCD matrix method is developed and used for the final loss value fitting. Experimentally, a cavity with extinction ratio over –70 dB and quality factor $Q = 1.02\times10^6$ is realized. The fitting results show a waveguide loss of 0.24 ± 0.01 dB/cm and a grating loss of 0.31 ± 0.01 dB/cm. These results are obtained with relatively high index contrast ($\Delta n > 0.001$) gratings with 0.1-pm wavelength scanning resolution. It is expected that with better design and wavelength scanning technique, this approach is applicable more generally to measure waveguide loss coefficients as low as 0.001 dB/cm.**

***Index Terms*—Optical planar waveguides, gratings, waveguide filters, optical losses.**

## I. Introduction

Low loss dielectric waveguides are critical for many applications in integrated photonics. Several groups have demonstrated low propagation loss waveguides [1]–[10]. In fact, losses as small as 0.1 dB/m and 0.9 dB/m have now been reported in weakly and strongly confined waveguides, respectively [3], [5], [11]. Ultra-low losses in long waveguides ($> 1$ m) have been measured using a coherent optical frequency domain reflectometry technique [3], [5]. The waveguides with losses less than 0.1 dB/m were fabricated by wafer bonding a thermal oxide layer as the upper cladding and resulted in a waveguide with ultra-low confinement and reduced scattering losses at the core-cladding interfaces [3]. Ring resonators with high quality factor $Q > 10^6$ have also been fabricated in low loss waveguides and often have been used to extract the loss coefficient in these waveguides [4], [11]–[13]. Applications of ultra-low loss waveguides are envisioned in optical gyroscopes [14]–[16], dispersion compensation [17], in packet-switched networks [18], optical filters [19]–[22], optomechanical sensing [4], [11], [23], [24] and in astrophotonics [25]–[30].

The major sources of loss in waveguides are material absorption, bending loss, and light scattering. An efficient and reliable method to measure these losses is critical for the design of many photonic integration applications. In the past decades, the most used loss measurement techniques are based on either length variation method (fabricating waveguides of different lengths) or ring resonator method (deriving waveguide loss from its relationship with cavity *Q*). In this work, we have developed a new approach for characterizing small losses in highly transparent $Si_3N_4/SiO_2$ waveguides on silicon. It relies on measuring the transmission of an on-chip Fabry-Perot (FP) cavity formed by two Bragg gratings and a straight waveguide between them. Indeed, additional scattering loss will be introduced by these Bragg gratings. However, with a proper design, it does not compromise loss measurement accuracy (see Section V-A). Compared with the length variation method, this approach is particularly applicable to waveguides written by EBL whose lengths cannot be easily extended beyond several centimeters. Compared with the ring resonator method, this approach uses a FP cavity which is formed on a straight structure. Therefore it does not involve bending loss, and can operate equally well for optical modes with any confinement factor. Moreover, different with other loss measurement methods based on FP cavity [31], [33], we use highly reflective ($R > 0.999$) integrated gratings as the cavity mirror and a more precise numerical fitting procedure, which gives much higher loss measurement accuracy (around 0.01 dB/cm in our experiment).

The paper is organized as follows: Section II discusses waveguide design and fabrication. In Section III, the physics model and theoretical fitting process are introduced. In Section IV, we first measure waveguide propagation loss by analyzing several $Si_3N_4/SiO_2$ waveguides of different lengths. After recognizing the limitation of this approach, we characterize the waveguide loss again using our new approach. In Section V, we demonstrate

Manuscript received November 28, 2017; revised April 3, 2018; accepted April 3, 2018. Date of publication April 16, 2018; date of current version May 18, 2018. This work was supported in part by W. M. Keck Foundation, and in part by the National Science Foundation under Grant AST1711377. *(Corresponding author: Mario Dagenais.)*

Y.-W. Hu, Y. Zhang, and M. Dagenais are with the Department of Electrical and Computer Engineering, University of Maryland, College Park, MD 20742 USA (e-mail: yiwenhu@umd.edu; yzhangdd@umd.edu; dage@umd.edu).

P. Gatkine is with the Department of Astronomy, University of Maryland, College Park, MD 20742 USA (e-mail: pgatkine@astro.umd.edu).

S. Veilleux is with the Department of Astronomy, University of Maryland, College Park, MD 20742 USA, and also with the Joint Space-Science Institute, University of Maryland, College Park, MD 20742 USA (e-mail: veilleux@astro.umd.edu).

J. Bland-Hawthorn is with the Sydney Institute for Astronomy, School of Physics, University of Sydney, Sydney, NSW 2006, Australia (e-mail: jbh@physics.usyd.edu.au).

Color versions of one or more of the figures in this paper are available online at http://ieeexplore.ieee.org.

Digital Object Identifier 10.1109/JSTQE.2018.2827663

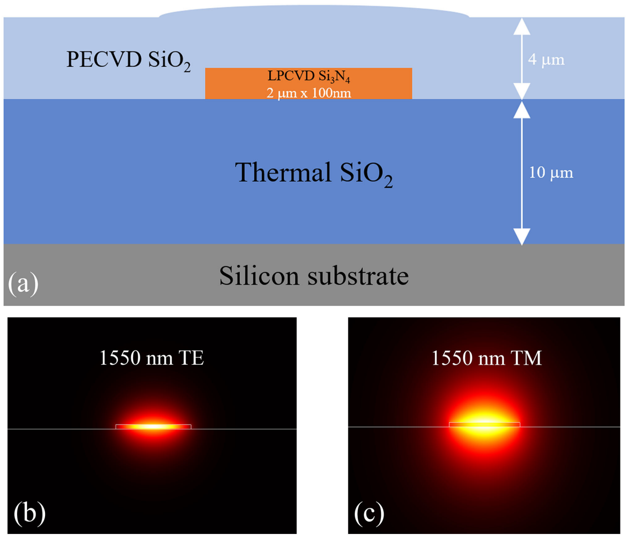


Fig. 1. (a) Waveguide cross section illustration (dimensions are not to scale). (b) TE mode profile at 1550 nm. (c) TM mode profile at 1550 nm.

by simulation that millimeter-length structures are enough to measure losses down to 0.01 dB/cm. A further factor of 10 improvement (0.001 dB/cm) is achievable with a centimeter-scale length. We summarize our main results in Section VI.

## II. Waveguide Design and Fabrication

### A. Waveguide Core Design

As shown in Fig. 1(a), our waveguide core is formed by 2 $\mu$m $\times$ 100 nm low pressure chemical vapor deposition (LPCVD) $Si_3N_4$. This core dimension is chosen for getting a reasonably confined mode with acceptable propagation loss. In general, thinner and wider core sizes are preferred for achieving lower loss waveguides [8]. However, those modes tend to have a small confinement factor, especially in the vertical direction, which makes them less attractive in applications requiring bends of small radii of curvature. For example, in arrayed waveguide gratings (AWGs), large bending radii of arrayed waveguides will make the device footprint increase appreciably [27], [34]. Therefore, we choose 100 nm as a trade-off value for the $Si_3N_4$ thickness. Additionally, 2 $\mu$m width is selected to ensure operation in single mode at a wavelength of 1.4 $\mu$m and above.

### B. Fabrication

In this paper, we use 10 µm thick thermal oxide to effectively reduce substrate leakage to the silicon substrate. The waveguides are patterned by 20kV Raith e-Line e-beam system with PMMA resist. After development, we use a liftoff process to form a reverse Chromium (Cr) mask. The mask is used for etching down $Si_3N_4$ by Inductively Coupled Plasma (ICP) Etching. Lastly, we remove the Cr and deposit 4 $\mu$m plasma-enhanced chemical vapor deposition (PECVD) oxide layer as the upper cladding.

We use EBL to write the full structure, which can be 1-3 cm long, the challenge of which can be classified into two categories. The first category is to reduce the sidewall roughness caused by unstable writing conditions which introduces scattering loss. The second category is to minimize horizontal and vertical offset (especially gaps) between e-beam write-fields (WFs) caused by alignment limitations, which can bring stitching loss.

Much work has been done to obtain ultra-low losses by focusing on reducing loss of the first category [11], [35]. However, for long waveguide gratings involving several ten to hundred WFs [25], the second issue can also be extremely critical. The reason is that it brings not only additional loss, but it also leads to accumulation of phase errors, which could lead to failure of the entire grating. In our experiment, to handle this issue appropriately, we first measure the stitching error in SEM and then use a proper WF zoom factor to minimize any possible gaps between the WFs. Moreover, we use Raith e-Line's Height Sensing function to dynamically control the beam focus point when moving from one WF to another during exposure. With the above two methods, we can achieve a decent loss level around 0.31 dB/cm for the grating and 0.24 dB/cm for the uniform waveguide, which will be discussed thoroughly in Section IV.

## III. Bragg Grating Modeling and Design

On-chip gratings are important for various photonic applications, such as sensing, filters and lasers. Among different types of gratings, Bragg gratings is one of the most promising candidates to be generally employed in photonic integrated circuits (PICs), mostly for its simplicity and compatibility with uniform waveguides. On the other hand, when it comes to the ultra-low loss regime, their extra scattering loss poses a challenge for researchers to make them competitive with their ring resonator counterparts.

In this work, we aim at using Bragg gratings to implement high reflectivity, low loss cavities: phase-shifted Bragg gratings (PSBG) and Bragg grating Fabry-Perot cavities (BGFP). Furthermore, we demonstrate how to use them as a characterization tool for low loss waveguides. In this section, we will first focus on their modeling and design.

Our theoretical model is based on the ABCD matrix method which is convenient to use for studying the transmission of optical waves in periodic structures. We will briefly discuss it, and a detailed theory can be found in [36]. What we consider here are two Bragg gratings with a physical cavity length $L_0$ in the center, as illustrated in Fig. 2(a). In the design, the grating on each side consists of $N$ pairs of alternating width ($w_1$ and $w_2$) waveguide segment with period $\Lambda = \lambda_c / 2n_{\mathrm{eff}}$. $\lambda_c$ is the stop-band center wavelength. Starting from basic electromagnetic equations, we can derive a matrix equation relating the field amplitude at two neighboring grating periods,

$$\begin{bmatrix} a_{n-1} \\ b_{n-1} \end{bmatrix} = \begin{bmatrix} A & B \\ C & D \end{bmatrix} \times \begin{bmatrix} a_n \\ b_n \end{bmatrix}$$

Here $a_{\mathrm{n}}$ and $b_{\mathrm{n}}$ are the electric field amplitude in the $nth$ grating period for a right-traveling and a left-traveling plane wave. Note that the ABCD coefficients are determined by the electrical boundary conditions. For the uniform cavity part,

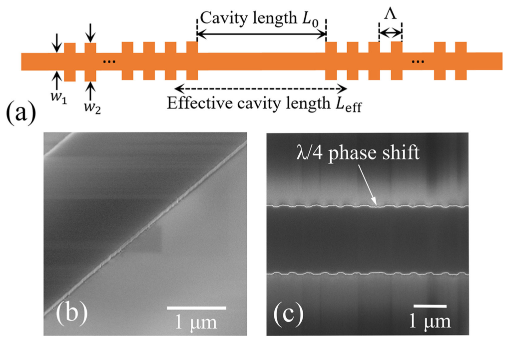


Fig. 2. (a) Illustration of the Bragg grating design. For PSBG, cavity length $L_0 = \Lambda \sim 550$ nm. For BGFP, we made the cavity length $L_0 = 1$ mm, 3 mm and 6 mm. (b) Tilted view of the 2 $\mu$m $\times$100 nm straight waveguide. (c) Top view of the λ/4 PSBG; the $\pi$ phase shifted part can be recognized in the figure center.

$A = e^{ik_{1z}L_0/2}$, $B = C = 0$, $D = e^{-ik_{1z}L_0/2}$. Here $k_{1z}$ is the propagation constant in width $w_1$ waveguide segment.

The coupling coefficient $\kappa$ is an important concept in coupled mode theory, which is quite useful for grating design [37]. For a 1-d grating discussed here, if we denote the larger index as $n_1$ and smaller index as $n_2$, $\kappa$ can be roughly estimated as $\kappa = \pi/\lambda$ $(n_1 - n_2)$, and the stopband width is [34]

$$\Delta\lambda \sim \frac{\lambda^2 \, |\kappa|}{\pi n_{eff}} \tag{1}$$

For the transmission calculation, we still need to know the effective indices for waveguide width $w_1$ and $w_2$ throughout the studied spectral range, which are obtained using the FIMMWAVE full-vectorial mode solver. Note that in the final fitting of the transmission curve, we still need to slightly adjust the index profile to account for the rounded edges of the grating structure [see Fig. 2(c)].

### A. $\pi$ Phase Shifted Bragg Grating

First we design a $\pi$ (i.e., λ/4) PSBG ($L_0 = \Lambda$) to get a narrow peak at the stopband center. The peak's linewidth and intensity are very sensitive to propagation loss, so we can use it to measure the grating loss $\alpha_{\rm g}$. To get high enough measurement resolution for state-of-the-art low loss waveguides, we want to design a PSBG with as narrow linewidth as possible, which requires a large $\kappa L_g$ for high reflection, where $L_g = N\Lambda$ is the grating length. After careful theoretical and empirical studies, we choose $w_1 = 2\,\mu$m, $w_2 = 2.15\,\mu$m, corresponding to a moderate $\kappa \sim 10\,\text{cm}^{-1}$, which is a compromise for low scattering loss and decent grating coupling efficiency. As $R \sim tanh^2(\kappa L_g)$, in the layout design, we choose $L_g$ to be around 3.5 mm to make $\kappa L_g$ large enough to get single side mirror reflection $R > 0.999$.

### B. Bragg Grating Fabry-Perot cavity

The $Q$ of PSBG is dominated by grating loss $\alpha_{\rm g}$. In order to measure uniform waveguide loss, we keep the same reflecting gratings and make $L_0$ much larger to form a Fabry-Perot cavity. Since the cavity loss is always smaller than the grating loss, photons will stay inside for longer time before leaking out. As a result, BGFP can have higher $Q$ ($Q \sim \omega\tau$, $\tau$ is the photon lifetime) than PSBG. This is confirmed experimentally in the next section.

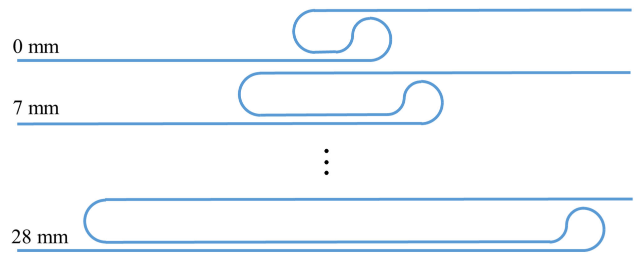


Fig. 3. Illustration of the bending waveguide design for measuring linear propagation loss. We made five waveguides on the chip with length difference of 0, 7, 14, 21, and 28 mm. The corresponding loss results are shown in Fig. 4.

### C. Loss Terms in the Model

Transmission matrix terms, A, B, C, D depends on 3 variables, $k_{1z}$, $k_{2z}$ (propagation constant in width $w_2$ waveguide segment), and the grating period $\Lambda$. To take the loss terms into consideration, we only need to add an imaginary part to $k_{1z}$ and $k_{2z}$. For example,

$$k_{1z} = n_1 \times \frac{2\pi}{\lambda} - in_{img} \times \frac{2\pi}{\lambda} \tag{2}$$

Note that $\alpha = 4\pi n_{\rm img}/\lambda$, and we have two loss terms, the grating loss $\alpha_g$ and the cavity loss $\alpha_c$ (for PSBG, $\alpha_{\rm c} = \alpha_{\rm g}$). By fitting our experimental and theoretical curve with different lengths cavities, we can extract both $\alpha_g$ and $\alpha_c$.

## IV. Experimental Results

To characterize the transmission spectrum, we use a setup composed of a Keysight 81600B tunable laser and a Keysight N7744A power meter. The tunable laser triggers the power meter during the wavelength scanning for fast spectral measurement with 0.1 pm resolution. Polarization maintaining fibers are used for optical mode launch and collection. Fiber rotators are also employed for the TE/TM control. The fiber input and output coupling are accomplished by two Newport VP-25XL XYZR motorized stages with 10 nm minimum incremental motion.

### A. Uniform Waveguide

We first measure the waveguide loss with uniform waveguides of different lengths. Two broadband sources centered at 1310 and 1550 nm are deployed to characterize the loss from 1200 to 1630 nm. The layout design is shown in Fig. 3, the length difference among them is 0, 7, 14, 21, and 28 mm. The extracted loss results are shown in Fig. 4.

The lowest loss occurs at the longer wavelength of the spectrum in Fig. 4. Specifically, at 1630 nm, the TE loss is 0.16 $\pm$ 0.18 dB/cm, and the TM loss is 0.32 $\pm$ 0.13 dB/cm. However, when we move to a shorter wavelength like 1558 nm, TE loss is 0.68 $\pm$ 0.25 dB/cm, and TM loss is 0.79 $\pm$ 0.20 dB/cm.

Two strong absorption peaks can be observed around 1390 nm and 1505 nm. Previous studies have noticed them in $Si_3N_4/SiO_2$

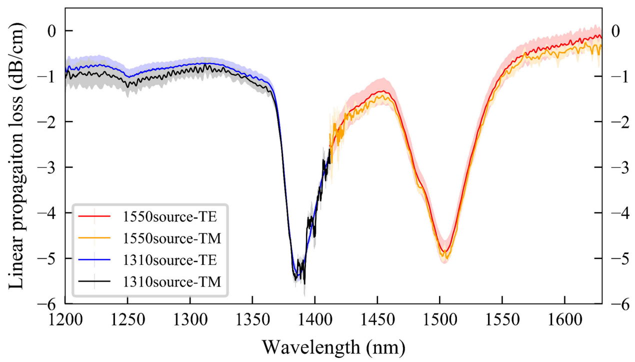


Fig. 4. Linear propagation loss of $Si_3N_4/SiO_2$ waveguide before annealing, extracted from the sample in Fig. 3. The error bars are shown as the shaded area.

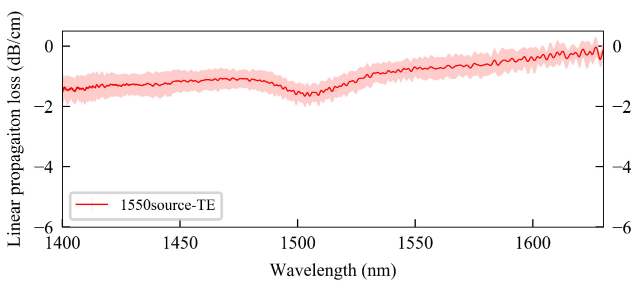


Fig. 5. TE propagation loss after annealing. The measurement is done with the same sample in Fig. 4, after 2 hour annealing in 1150C.

platforms [38], [39], and they are generally attributed to O-H, N-H, Si-H bonds in the two materials. These peaks can be largely removed by annealing at high temperature, as shown in Fig. 5. It can also be seen that the measurement error increased after annealing. A possible reason is that the annealing process introduced larger coupling efficiency fluctuation among different waveguides. This is also a main disadvantage of this loss measurement method, whose measurement error depends not only on the waveguide fabrication stability, but also on the coupling efficiency stability.

### B. $\pi$ Phase Shifted Bragg Grating

As we can see, the previous method shows a measurement error of at least 0.1 dB/cm, which is undesirable for current low loss waveguide. Now we used two PSBG to demonstrate the loss fitting at two different wavelengths, 1558 and 1629 nm, and compare with the loss obtain in IV. A.

The fitting process is as follows: first, we scale and shift the index profile to fit the stopband position and width; next we adjust grating loss $\alpha_g$ to find the best fitting curve, as shown in Fig. 6. The fitting parameters are also shown in the caption. An important criteria is that we must use the same wavelength dependent effective index profile for the fitting curves. The 1558 nm PSBG has a larger index contrast than the 1629 nm PSBG because the shorter wavelength mode is more confined and more sensitive with width variation.

From the theoretical fit, we get grating loss $\alpha_g = 0.64$ dB/cm at 1558 nm and $\alpha_g = 0.31$ dB/cm at 1629 nm. Although we only

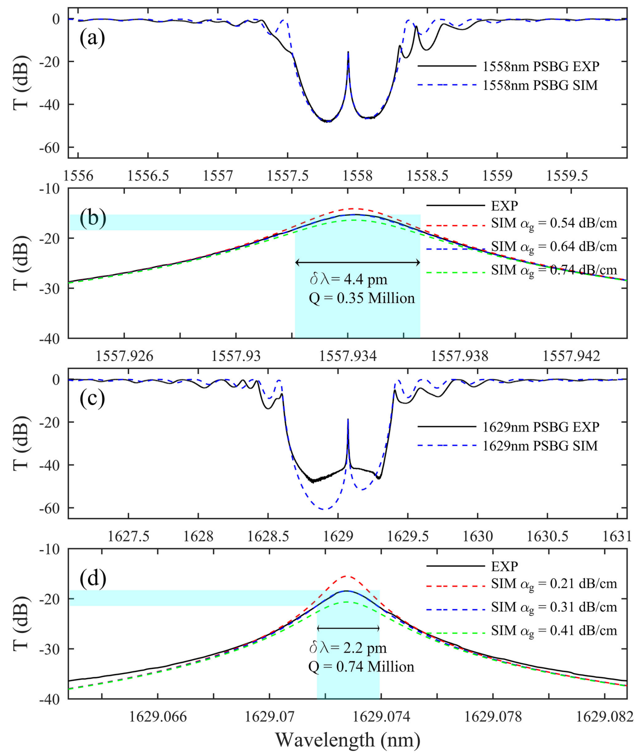


Fig. 6. PSBG grating experimental (black solid line) and theoretical fitting (dashed lines) results. In (a) and (c), the wavelength range is 4 nm. In (b) and (d), the wavelength range is 20 pm. Fitting parameters: (1558 nm) $n_1 = 1.47584$, $n_2 = 1.47691$; $\Delta n = 0.00107$, $\kappa = 10.81\ \mathrm{cm}^{-1}$, stopband width $\Delta\lambda = 0.563$ nm. (1629 nm) $n_1 = 1.47171$, $n_2 = 1.47273$; $\Delta n = 0.00102$, $\kappa = 9.85\ \mathrm{cm}^{-1}$, $\Delta\lambda = 0.561$ nm.

TABLE I
PSBG (Centered at 1629 nm) Fine Fitting Results for Fig. 6

| $L_0$ | Loss [dB/cm] | Center Peak intensity [a] | Linewidth [b] | $Q$ |
|---|---|---|---|---|
| 553 nm (=Λ) | 0.29 | -17.95 dB | 2.06 pm | $7.90 \times 10^5$ |
| | 0.31 | -18.47 dB | 2.19 pm | $7.45 \times 10^5$ |
| | 0.33 | -18.96 dB | 2.31 pm | $7.05 \times 10^5$ |

[a] The center peak intensity is the maximum transmission the center peak can reach. The center peak intensity will be exactly 0 dB if both the grating loss $\alpha_g$ and cavity loss $\alpha_c$ are 0.

[b]The linewidth measured in experiment is 2.2 pm.

plotted another two fitting curves with $\pm$ 0.1 dB/cm in Fig. 6, the fitting accuracy can actually reach about $\pm$ 0.01 dB/cm with 0.1 pm wavelength resolution, as shown in Table I.

For the 1629 nm PSBG, the narrowest linewidth we can get is 2.2 pm, corresponding to a $Q \sim 7.4 \times 10^5$. The extinction ratio (ER) of the 1558 nm grating is 50 dB, and that of the 1629 nm grating is 60 dB (limited to 50 dB in measurement by the uncoupled fiber input light). It implies a single side mirror reflection $R \sim 0.999$ around 1629 nm.

### C. Bragg Grating Fabry-Perot Cavity

We can extract the grating loss from the PSBG sample. However, we still cannot tell the exact straight waveguide

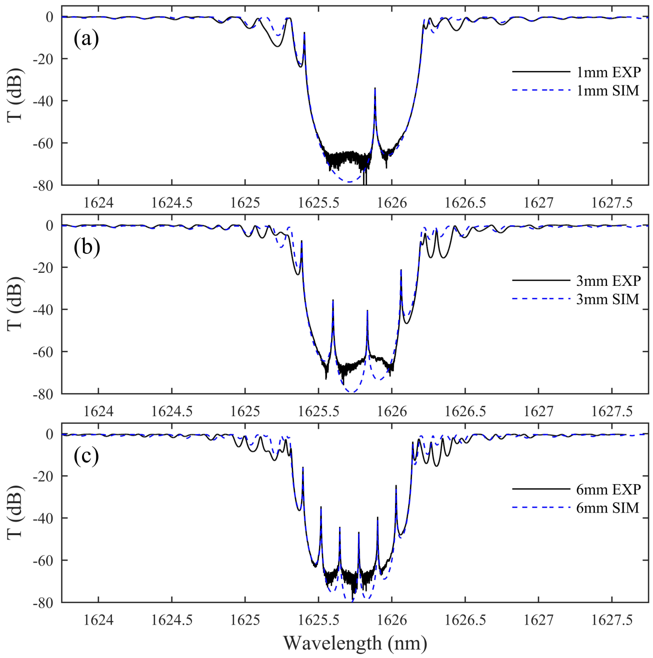

Fig. 7. Experimental and simulation curves for Bragg grating cavity with length (a) 1 mm, (b) 3 mm and (c) 6 mm. For the blue simulation curve, we use grating loss 0.41 dB/cm and cavity (straight waveguide) loss 0.24 dB/cm. The wavelength range is 4 nm in all four panels. The *y* axes are set to be the same. Fitting parameters: $n_1 = 1.47860$, $n_2 = 1.47979$; $\Delta n = 0.00119$, $\kappa = 11.5\,\mathrm{cm}^{-1}$, $\Delta\lambda = 0.649\,\mathrm{nm}$.

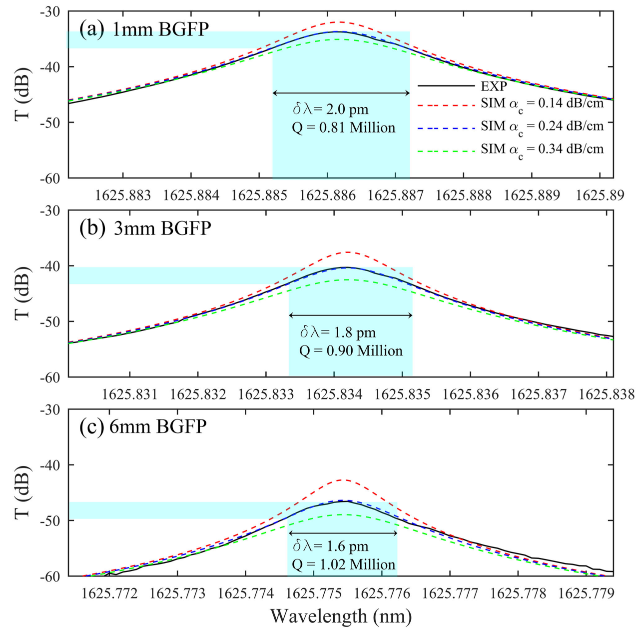

Fig. 8. The enlarged figure for BGFP transmissions. Red, blue and green lines denotes cavity loss $\alpha_c = 0.14$ dB/cm, 0.24 dB/cm and 0.34 dB/cm. Grating loss $\alpha_g$ is set as 0.4 dB/cm. (a) 1 mm cavity with linewidth 2.0 pm. (b) 3 mm cavity with linewidth 1.8 pm. (c) 6 mm cavity with linewidth 1.6 pm. Note that the legend in (a) also holds for (b) and (c). The *x* range are all 8 pm, *y* axes are set to be the same.

loss. We fabricated three additional Bragg gratings with center length 1 mm, 3 mm and 6 mm. Thus, the transmission contains the information from both $\alpha_g$ and $\alpha_c$. The fitting process is similar to that of the PSBG, and the results are shown in Fig. 7.

In this BGFP sample we kept the grating design parameters the same as for the PSBG sample. However, ER can reach $-70$ dB in experiment and $-80$ dB by fitting. A one-side mirror reflectivity $R \sim 0.9999$ is achieved. There are two reasons that we get higher ER than in Fig. 6. First, we increase the offset between the input and the output waveguides to reduce the background light intensity; secondly, we have higher index contrast $\Delta n$ due to a slightly thicker LPCVD $Si_3N_4$ layer, which can be confirmed in the $\Delta n$ fitting parameters (0.00119 vs 0.00102).

In the enlarged plots of Fig. 8, it can be seen clearly that the longer cavity leads to a narrower linewidth, consistent with our expectations. The best $Q$ we get is $1.02 \times 10^6 \sim \delta\lambda = 1.6\,\mathrm{pm}$. To our knowledge, this is the best $Q$ obtained with on-chip Bragg gratings. From Table II, we can see that the resolution is still around $\pm$ 0.01 dB/cm.

We also studied the effective cavity length $L_{\mathrm{eff}}$ [illustrated in Fig. 2(a)] of BGFP. From Fig. 7, we measured the FSR for each cavity. They are 0.481 nm, 0.234 nm and 0.129 nm, which corresponds to $L_{\mathrm{eff}} = 1.86\,\mathrm{mm}$, 3.82 mm and 6.93 mm, respectively. The difference between $L_{\mathrm{eff}}$ and $L_0$ is quite stable, about 0.8-0.9 mm, which is favorable to design specific FSR cavities.

TABLE II
BGFP (CENTERED AT 1625.8 NM) FINE FITTING RESULTS FOR FIG. 8

| $L_0$ | Loss [dB/cm] | Center Peak intensity [a] | Linewidth [b] | $Q$ |
|---|---|---|---|---|
| 6 mm | 0.22 | -45.78 dB | 1.51 pm | $1.08 \times 10^6$ |
| | 0.24 | -46.40 dB | 1.62 pm | $1.00 \times 10^6$ |
| | 0.26 | -46.98 dB | 1.73 pm | $0.94 \times 10^6$ |

[a] Modeling uses $\alpha_g$ = 0.41 dB/cm.
[b] The experimental linewidth is 1.6 pm.

## V. FURTHER DISCUSSIONS

### A. *Loss Reduction*

As shown in Fig. 2(b), there exists some obvious roughness along waveguide boundaries, which is our device's dominant loss source. The roughness comes from e-beam lithography and lift-off process, but the latter probably plays a more important role. In future work, we plan to use lift-off resist (LOR) or a negative resist [11] to reduce the edge roughness and thereafter the loss.

Another loss term in our measurement is the scattering loss due to mode mismatch at the interface between the straight waveguide and the grating. This loss will become more influential if higher width contrast grating is used. However, it can

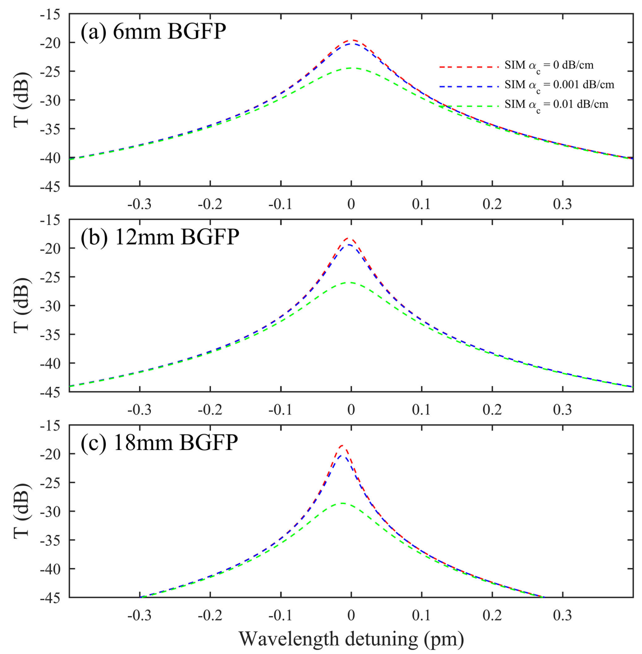


Fig. 9. BGFP simulation to demonstrate its potential for measuring very low loss coefficients. We keep the grating loss $\alpha_g = 0.1$ dB/cm, and set the cavity loss $\alpha_c = 0, 0.001$ and 0.01 dB/cm.

be virtually eliminated by reducing the sidewall modulation to zero at these interfaces.

### B. Lower Limit of Measurable Waveguide Loss

Considering the fact that people have already achieved losses down to 0.001 dB/cm similar platforms [11], it is quite important to assess our approach's lower limit of measurable loss.

Since our $\alpha_g$ can be 0.31 dB/cm, only 0.07 dB/cm higher than the straight waveguide loss, it is reasonable to assume that our current Bragg grating design introduces an extra scattering loss $< 0.1$ dB/cm. Now we can simulate whether our approach is applicable for the current best waveguide loss level $\sim 0.001$ dB/cm [3], [11].

In Fig. 9, we keep $\alpha_g = 0.1$ dB/cm, and set $\alpha_c$ as 0, 0.001 and 0.01 dB/cm. If we look at the green curve, which stands for 0.01 dB/cm loss level, it is obvious that our approach can easily handle it even with cavity length 6 mm. For 0.001 dB/cm loss, however, we may have to use longer cavities to increase the sensitivity. In Table III, we exhibited some numerical values extracted from Fig. 9. For a 12 mm BGFP with $\alpha_c = 0.001$ dB/cm, although the linewidth only changes by 0.006 pm compared with $\alpha_c = 0$ dB/cm, the center peak intensity can drop more than 1 dB, which can easily be measured in the experiment without much difficulty. This result implies that we can still characterize the waveguide loss, even if it is much lower than the grating loss. The reason is that we can always try to increase the number of grating periods to achieve high enough reflection so that the cavity transmission becomes adequately sensitive within the expected waveguide loss range.

TABLE III
12 MM BGFP MODELING RESULTS RELATED WITH FIG. 9

| $L_0$ | Loss [dB/cm][a] | Center Peak intensity | Linewidth | $Q$ |
|---|---|---|---|---|
| 12 mm | 0 | -18. 29 dB | 0.041 pm | $3.97 \times 10^7$ |
| | 0.001 | -19.45 dB | 0.047 pm | $3.46 \times 10^7$ |
| | 0.01 | -26.01 dB | 0.100 pm | $1.63 \times 10^7$ |

[a] Modeling uses grating loss 0.1 dB/cm.

### C. Lower $\kappa$ Grating

Another direction to optimize our approach is to use a lower $\kappa$ grating for getting lower $\alpha_g$. Now our grating $\kappa$ is about $10\,\text{cm}^{-1}$. If we decrease it and increase $L_g$ to keep $\kappa L_g$ a constant, we will also see an improvement in the loss measurement limit.

The underlying physics is that for the center cavity, its peak linewidth $\delta\lambda$ depends only on the loss terms $\alpha_g$, $\alpha_c$, $L_{\text{eff}}$ and grating reflection $\kappa L_g$. As long as $\kappa$ drops and we extend $L_g$ to keep the mirror reflectivity the same, the cavity $Q$ will be increased. In experiment, a 1/10 factor decrease ($\kappa = 1\,\text{cm}^{-1}$) is definitely achievable [20]. Further reduced grating $\kappa$ might be limited by fabrication stability and accuracy.

### D. Loss Measurement Bandwidth

Since we use a simple Bragg grating as a reflective mirror, there is only one stopband in the wavelength range of interest and the bandwidth is also quite narrow. To measure losses at different position, we have to use multiple waveguides or multiple cavities in a line. However, combined with the complex grating technologies we developed for on-chip waveguides [25] or fibers [30], the proposed approach is actually quite viable to be used for loss measurement with over 100 nm wavelength range. This is very attractive for ultra-fast, ultra-broadband loss characterization.

## VI. CONCLUSION

We have proposed an alternative method for measuring ultra-low loss coefficients in a waveguide, which is both accurate and efficient. We have also demonstrated on-chip Bragg grating cavities with $Q = 1.02 \times 10^6$, which as far as we are concerned is the highest experimentally observed Bragg grating cavity $Q$. The straight waveguide loss measured with this new approach is $0.24 \pm 0.01$ dB/cm. The loss measurement limit and accuracy generally scales with the grating and waveguide loss, making this approach promising to measure waveguide loss down to 0.001 dB/cm.

## ACKNOWLEDGMENT

The authors would like to thank Dr. T. Zhu and UMD Ph.D. student S. Xie for constructive discussions, and also acknowledge the support of the Maryland NanoCenter and its AIMLab.

## REFERENCES


[1] R. Adar, M. R. Serbin, and V. Mizrahi, "Less than 1 dB per meter propagation loss of silica waveguides measured using a ring resonator," *J. Lightw. Technol.*, vol. 12, no. 8, pp. 1369–1372, Aug. 1994.

[2] B. Little, "A VLSI Photonics Platform," in *Proc. Opt. Fiber Commun. Conf.*, 2003, Paper ThD1.

[3] J. F. Bauters *et al.*, "Planar waveguides with less than 0.1 dB/m propagation loss fabricated with wafer bonding," *Opt. Express*, vol. 19, no. 24, pp. 24090–24101, Nov. 2011.

[4] H. Lee *et al.*, "Chemically etched ultrahigh-Q wedge-resonator on a silicon chip," *Nat. Photon.*, vol. 6, no. 6, pp. 369–373, Jun. 2012.

[5] H. Lee, T. Chen, J. Li, O. Painter, and K. J. Vahala, "Ultra-low-loss optical delay line on a silicon chip," *Nature Commun.*, vol. 3, May 2012, Art. no. 867.

[6] D. J. Moss, R. Morandotti, A. L. Gaeta, and M. Lipson, "New CMOS-compatible platforms based on silicon nitride and Hydex for nonlinear optics," *Nature Photon.*, vol. 7, no. 8, pp. 597–607, Aug. 2013.

[7] M. J. R. Heck, J. F. Bauters, M. L. Davenport, D. T. Spencer, and J. E. Bowers, "Ultra-low loss waveguide platform and its integration with silicon photonics," *Laser Photon. Rev*., vol. 8, no. 5, pp. 667–686, Sep. 2014.

[8] D. T. Spencer, J. F. Bauters, M. J. R. Heck, and J. E. Bowers, "Integrated waveguide coupled Si3N4 resonators in the ultrahigh-Q regime," *Optica*, vol. 1, no. 3, pp. 153–157, Sep. 2014.

[9] K. Wörhoff, R. G. Heideman, A. Leinse, and M. Hoekman, "TriPleX: A versatile dielectric photonic platform," *Adv. Opt. Technol.*, vol. 4, no. 2, pp. 189–207, 2015.

[10] M. Belt, M. L. Davenport, J. E. Bowers, and D. J. Blumenthal, "Ultra-low-loss Ta2O5-core/SiO2-clad planar waveguides on Si substrates," *Optica*, vol. 4, no. 5, pp. 532–536, May 2017.

[11] X. Ji *et al.*, "Ultra-low-loss on-chip resonators with sub-milliwatt parametric oscillation threshold," *Optica*, vol. 4, no. 6, pp. 619–624, Jun. 2017.

[12] Q. Li, A. A. Eftekhar, M. Sodagar, Z. Xia, A. H. Atabaki, and A. Adibi, "Vertical integration of high-Q silicon nitride microresonators into silicon-on-insulator platform," *Opt. Express*, vol. 21, no. 15, pp. 18236–18248, Jul. 2013.

[13] K. Luke, A. Dutt, C. B. Poitras, and M. Lipson, "Overcoming Si3N4 film stress limitations for high quality factor ring resonators," *Opt. Express*, vol. 21, no. 19, pp. 22829–22833, Sep. 2013.

[14] C. Ciminelli, F. Dell'Olio, C. E. Campanella, and M. N. Armenise, "Photonic technologies for angular velocity sensing," *Adv. Opt. Photon.*, vol. 2, no. 3, pp. 370–404, Sep. 2010.

[15] S. Srinivasan, R. Moreira, D. Blumenthal, and J. E. Bowers, "Design of integrated hybrid silicon waveguide optical gyroscope," *Opt. Express*, vol. 22, no. 21, pp. 24988–24993, Oct. 2014.

[16] T. Huffman, M. Davenport, M. Belt, J. E. Bowers, and D. J. Blumenthal, "Ultra-low loss large area waveguide coils for integrated optical gyroscopes," *IEEE Photon. Technol. Lett.*, vol. 29, no. 2, pp. 185–188, Jan. 2017.

[17] R. Moreira, S. Gundavarapu, and D. J. Blumenthal, "Programmable eye-opener lattice filter for multi-channel dispersion compensation using an integrated compact low-loss silicon nitride platform," *Opt. Express*, vol. 24, no. 15, pp. 16732–16742, Jul. 2016.

[18] E. F. Burmeister *et al.*, "Photonic integrated circuit optical buffer for packet-switched networks," *Opt. Express*, vol. 17, no. 8, pp. 6629–6635, Apr. 2009.

[19] T. Huffman, D. Baney, and D. J. Blumenthal, "High extinction ratio widely tunable low-loss integrated Si3N4 third-order filter," arXiv:1708.06344., Aug. 2017.

[20] D. T. Spencer, M. Davenport, S. Srinivasan, J. Khurgin, P. A. Morton, and J. E. Bowers, "Low kappa, narrow bandwidth Si3N4 Bragg gratings," *Opt. Express*, vol. 23, no. 23, pp. 30329–30336, Nov. 2015.

[21] T. Komljenovic and J. E. Bowers, "Monolithically integrated high-Q Rings for narrow linewidth widely tunable lasers," *IEEE J. Quantum Electron.*, vol. 51, no. 11, pp. 1–10, Nov. 2015.

[22] J. F. Bauters, J. R. Adleman, M. J. R. Heck, and J. E. Bowers, "Design and characterization of arrayed waveguide gratings using ultra-low loss Si3N4 waveguides," *Appl. Phys. A*, vol. 116, no. 2, pp. 427–432, Aug. 2014.

[23] Y.-W. Hu, Y.-F. Xiao, Y.-C. Liu, and Q. Gong, "Optomechanical sensing with on-chip microcavities," *Frontiers Phys.*, vol. 8, no. 5, pp. 475–490, Oct. 2013.

[24] Y.-W. Hu, B.-B. Li, Y.-X. Liu, Y.-F. Xiao, and Q. Gong, "Hybrid photonic–plasmonic mode for refractometer and nanoparticle trapping," *Opt. Commun.*, vol. 291, pp. 380–385, Mar. 2013.

[25] T. Zhu, Y. Hu, P. Gatkine, S. Veilleux, J. Bland-Hawthorn, and M. Dagenais, "Arbitrary on-chip optical filter using complex waveguide Bragg gratings," *Appl. Phys. Lett.*, vol. 108, no. 10, Mar. 2016, Art. no. 101104.

[26] T. Zhu, Y. Hu, P. Gatkine, S. Veilleux, J. Bland-Hawthorn, and M. Dagenais, "Ultrabroadband high coupling efficiency fiber-to-waveguide coupler using Si 3N4 /SiO2 waveguides on silicon," *IEEE Photon. J.*, vol. 8, no. 5, pp. 1–12, Oct. 2016.

[27] P. Gatkine, S. Veilleux, Y. Hu, J. Bland-Hawthorn, and M. Dagenais, "Arrayed waveguide grating spectrometers for astronomical applications: new results," *Opt. Express*, vol. 25, no. 15, pp. 17918–17935, Jul. 2017.

[28] J. Bland-Hawthorn and P. Kern, "Astrophotonics: A new era for astronomical instruments," *Opt. Express*, vol. 17, no. 3, pp. 1880–1884, Feb. 2009.

[29] S. G. Leon-Saval, A. Argyros, and J. Bland-Hawthorn, "Photonic lanterns: A study of light propagation in multimode to single-mode converters," *Opt. Express*, vol. 18, no. 8, pp. 8430–8439, Apr. 2010.

[30] J. Bland-Hawthorn *et al.*, "A complex multi-notch astronomical filter to suppress the bright infrared sky," *Nature Commun.*, vol. 2, pp. 581–587, 2011.

[31] R. G. Walker, "Simple and accurate loss measurement technique for semiconductor optical waveguides," *Electron. Lett.*, vol. 21, no. 13, pp. 581–583, Jun. 1985.

[32] T. Feuchter and C. Thirstrup, "High precision planar waveguide propagation loss measurement technique using a Fabry-Perot cavity," *IEEE Photon. Technol. Lett.* vol. 6, no. 10, pp. 1244–1247, Oct. 1994.

[33] A. Grieco, B. Slutsky, and Y. Fainman, "Characterization of waveguide loss using distributed Bragg reflectors," *Appl. Phys. B*, vol. 114, no. 4, pp. 467–474, Mar. 2014.

[34] W. Bogaerts *et al.*, "Compact wavelength-selective functions in silicon-on-insulator photonic wires," *IEEE J. Sel. Topics Quantum Electron.*, vol. 12, no. 6, pp. 1394–1401, Nov./Dec. 2006.

[35] R. J. Bojko, J. Li, L. He, T. B.-J., M. Hochberg, and Y. Aida, "Electron beam lithography writing strategies for low loss, high confinement silicon optical waveguides," *J. Vac. Sci. Technol. B*, vol. 29, no. 6, Oct. 2011, Art. no. 06F309.

[36] A. Yariv and P. Yeh, "Wave propagation in periodic media," in *Photonics: Optical Electronics in Modern Communications*, 6th ed. New York, NY, USA: Oxford Univ. Press, 2007, ch. 12.

[37] J. Bland-Hawthorn, A. Buryak, and K. Kolossovski, "Optimization algorithm for ultrabroadband multichannel aperiodic fiber Bragg grating filters," *J. Opt. Soc. Amer.*, vol. 25, no. 1, pp. 153–158, Jan. 2008.

[38] C. H. Henry, R. F. Kazarinov, H. J. Lee, K. J. Orlowsky, and L. E. Katz, "Low loss Si3N4-SiO2 optical waveguides on Si," *Appl. Opt.*, vol. 26, no. 13, pp. 2621–2624, Jul. 1987.

[39] M. J. Shaw, J. Guo, G. A. Vawter, S. Habermehl, and C. T. Sullivan, "Fabrication techniques for low-loss silicon nitride waveguides," *Proc. SPIE*, vol. 5720, pp. 109–118, Jan. 2005.


**Yi-Wen Hu** received two B.S. degrees in physics/computer software in 2011, and the M.S. degree in optics in 2014 from Peking University, Beijing, China. He is currently working toward the Ph.D. degree in electrical engineering at the University of Maryland, College Park, MD, USA.

From 2011 to 2014, he was a Research Assistant with Peking University focused on optical microcavities and optomechanical sensing. Since 2014, he has been a Research Assistant with the University of Maryland with interests in on-chip optical waveguides/gratings/cavities for applications in communications, quantum information, and astrophotonics. He was the recipient of Clark School of Engineering Distinguished Graduate Fellowship in 2014.

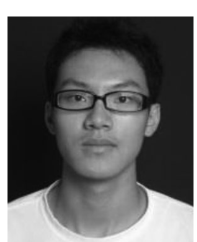

**Yang Zhang** received the B.S. degree in electrical engineering from Fudan University, Shanghai, China, in 2012. He is currently working toward the Ph.D. degree in electrical engineering at the University of Maryland, College Park, MD, USA.

His research interests include CIGS solar cell, optical phased array, and silicon nitride photonics.

**Pradip Gatkine** received the B.Tech. degree from the Indian Institute of Technology Bombay, Mumbai, India, in 2014, and the M.S. degree in astronomy from the University of Maryland, College Park, MD, USA, in 2016. He is currently working toward the Ph.D. degree in astronomy at the University of Maryland.

His photonic research focuses on the development of next generation of astrophotonic instrumentation for upcoming large telescopes. His current work involves the development of moderate resolution astrophotonic arrayed waveguide grating spectrographs and studying OH-suppression for astronomical telescopes. On the astrophysics side, he is interested in studying the early universe, especially using gamma-ray bursts as probes. He is currently working on studying the circumgalactic medium in the early universe. He is a member of the International Society of Optics and Photonics and American Astronomical Society.

**Sylvain Veilleux** received the B.S. degree in physics from the Université de Montréal, Montréal, QC, Canada, in 1984, and the Ph.D. degree in astronomy from the University of California, Santa Cruz, CA, USA, in 1989.

In 1995, he became an Assistant Professor with the Department of Astronomy, University of Maryland, College Park, MD, USA. He was promoted to Associate Professor in 2000 and to Full Professor in 2005. Since 2003, he has been the Optical Director at Maryland. He is the author of more than 200 refereed articles. His research interests include the physics of active galactic nuclei and starburst galaxies, particularly the connection between the supermassive black hole, the starburst, and the host galaxy, and the importance of feedback on galaxy evolution and the intracluster medium. He is also the lead on a number of instrumentation projects for large ground-based optical and near-infrared telescopes with applications for space missions and beyond.

Prof. Veilleux was an NSERC Fellow with the Institute for Astronomy, Honolulu, HI, USA, from 1989 to 1992, and a Hubble Fellow with the National Optical Astronomy Observatory, Tucson, AZ, USA, from 1992 to 1995. He is also a Fellow of the Joint Space-Science Institute. He was the recipient of the NASA Hubble Fellowship, the National Science Foundation CAREER Award, the Humboldt Prize, the John Simon Guggenheim Memorial Foundation Fellowship, and the Aspen Institute Italia Award.

**Joss Bland-Hawthorn** was born and educated in the U.K. From 1985 to 1988, he was a Postdoctoral Fellow with the Institute for Astronomy, Honolulu, HI, USA. He then served as a tenured Professor in physics with Rice University, Houston, TX, USA, before moving to Sydney, NSW, Australia, in 1993. From 2000 to 2007, he was the Head of Instrument Science Group, Anglo-Australian Observatory during where he established the fields of astrophotonics and galactic archaeology. With Birks and Leon-Saval, he developed the photonic lantern. He has authored or coauthored 550 research papers in optics, photonics, physics, astrophysics, and astronomical instrumentation. During the past decade, he was the recipient of the prestigious Federation and Laureate Fellowships. He was the recipient of many awards including the 2011 Jackson Gwilt Medal, the 2015 WH Steel Medal, the 2017 Thomas Ranken Lyle Medal, and the 2018 Miller Professorship to Berkeley. He is a Fellow of the Australian Academy of Science and the Optical Society of America. He is currently the Director of the Sydney Institute for Astronomy and an Assistant Director of the Institute of Photonics and Optical Science, University of Sydney, Sydney, NSW, Australia.

**Mario Dagenais** (F'10) received the Ph.D. degree in physics from the University of Rochester, Rochester, NY, USA, in 1978, working in quantum optics and photon correlations under the direction of Prof. Mandel. Together with J. Kimble, he made the first observation of photon antibunching. From 1978 to 1980, he was a Research Fellow with Harvard University, where he worked in nonlinear optics with Prof. N. Bloembergen. From 1980 to 1987, he worked with GTE Laboratories on photonic switching and semiconductor lasers. In 1987, he joined the University of Maryland, College Park, MD, USA, where he has been a Professor in electrical and computer engineering since 1991. He has more than 300 archival and conference publications. His research interests include $Si_3N_4/SiO_2$ integrated nanophotonic devices on Si, GaN light sources, and quantum dot GaAs/AlGaAs, CIGS, and perovskite photovoltaics. He is a Fellow of the Optical Society of America and a Fellow of the Electromagnetic Society.